International Conference on Artificial Reality and Telexistence
Eurographics Symposium on Virtual Environments (2023)
J.-M. Normand, M. Sugimoto, and V. Sundstedt (Editors)

3D Computer Graphics-Based Grass Pixel Simulation System for Color Scale Mapping Method

Akito Mizuno[1], Kojiro Tanaka[1], Masahiko Mikawa[2], Makoto Fujisawa[2]

[1]Graduate School of Comprehensive Human Sciences, University of Tsukuba, Ibaraki, Japan
[2]Institute of Library, Information and Media Science, University of Tsukuba, Ibaraki, Japan

Abstract

Recently, a wide range of media devices have been developed, with increasing emphasis on activities related to media art using natural elements. Although numerous studies have been conducted to harmonize media devices with natural landscapes, there is research on a display device using grass, termed artificial grass display, and its foundational element, artificial grass pixel. The artificial grass pixel employs the mechanism of pin displays and two types of grass to dynamically control the color of the grass. Moreover, studies are being conducted on the method of color scale mapping for the artificial grass pixel. However, there is a problem in experiments in the real space conditions due to the experimental overhead of acquiring a lot of data for color scale mapping. In order to solve this problem, this study aims to replicate and evaluate the artificial grass pixel in a virtual space using Computer Graphics (CG) technology. In this paper, we propose a novel method to estimate characteristic parameters of CG models based on a genetic algorithm to minimize the color difference from a real model. As a result, by performing calibration using multiple sets of real data, it was confirmed that the simulated grass pixel demonstrated color and color scale evaluation results aligned based on the color difference with the grass pixel in the real space.

CCS Concepts

• ***Computing methodologies*** → ***Modeling and simulation;***

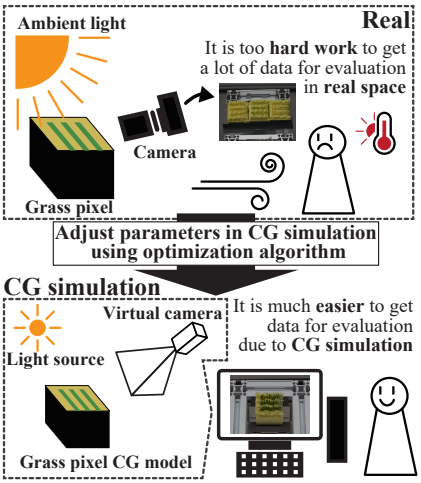

Figure 1: *The concept of this study. CG simulation reduces the experimental hardship and experiment time in the real space.*

1. Introduction

Public displays have become important, offering real-time information such as maps, weather updates, and time to the people. Consequently, they are now also found in green environments like parks [Ecl14]. However, most current media devices constituting these public displays employ liquid crystal displays (LCDs), raising concerns about their potential impact on the surrounding natural landscape [Sad14]. Therefore, there have been many studies of media devices and exhibits of artwork using natural materials familiar to our daily lives. For example, research on drawing with water [NMI*20], sand art [Dis15], and rice paddy art with different colored rice plants [Gov20]. Among these natural materials, grass materials that easily blend into the green environment are attracting attention. There is research on the grass display that uses grass and the grass pixel that makes up the grass display [TMF21]. The grass display is a media device of animated expression using artificial grass by dynamically controlling the green grass length against the fixed length of the yellow grass to produce color changes. Tanaka et al. have also proposed mapping the color scale of the grass pixel to the green grass length [TKM*23]. This method determines the color scale of the grass pixel based on the grass length through some experiments outdoors during the daytime for color evaluation. On the other hand, since the color scale mapping is based on the green grass length in the experiment, it is necessary to photograph the grass pixel for each target grass length and for each location to be observed. Therefore, it is hard work to acquire a lot of data and take a long time to conduct experiments and prepare for experiments.

In this paper, we propose a method of simulating the grass color

DOI: 10.2312/egve.20231307

mapping process of the grass pixel by using computer graphics (CG). A CG simulation for the grass pixel reproduces the colors measured by the grass pixel by setting up the grass pixel in the real space and ambient light. For the purpose of reproducing the grass pixel, we develop a system that can adjust parameters in the CG simulation using an optimization algorithm. Figure 1 illustrates the concept of this study, which allows users to check the color of the grass pixel and experiment with the color scale mapping by preparing the data needed to build the CG simulation from real space. The performance of the proposed CG simulation is evaluated by comparing the results of color difference and verifying whether the color scale mapping results obtained by the CG simulation are effective in controlling the color scale of the grass pixel in real space.

The contributions of this study are as follows.

- Construction of simulation for the grass pixel and real space environment.
- Reproduction of the color of the grass pixel in the CG space.
- Evaluation of the color scale mapping of the grass pixel in the CG space.

2. Related work

2.1. Media devices using natural materials

Media devices using natural materials have gained attention, and various methods employing materials such as water [NMI*20], sand [DWPF15, Dis15], fur [STH*14], and food [RPH*19] have been proposed. In addition, there has been research on media devices that use plants, a material that more naturally blends with natural landscapes. Examples of such research include 'Follow the Grass' by Minuto et al. [MN12], 'Grassffiti' by Sugiura et al. [STK*17], and 'Plantxel' by Gentile et al. [GSEM18], although these studies have not focused on animation displays.

We focus on the concepts of 'grass display' and 'grass pixel'. This concept was proposed by Tanaka et al. to achieve animation displays using artificial grass [TMF21]. They also proposed a mapping method for the color scale of the grass pixel in the animation display [TKM*23]. However, capturing the grass pixel with the grass length at regular intervals was required to conduct the color scale mapping. Thus, the experiment on the color scale mapping took a long time. In order to minimize the labor and time required for experiments of color scale mapping, we propose to reproduce the grass pixel and the experimental environment in the CG space. This approach has the potential to reduce the experimental burden in the real space by conducting experiments about color scale mapping of the grass pixel on a CG simulation.

2.2. Simulation using CG technology

Simulation using CG technology is applied to assist in the development process and in collecting user data. Studies have explored user experiences with cameras [MZS*19], comfort simulations for aircraft interiors [GL21], and methodologies for investigating users' lighting preferences [HPC*], suggesting a wide range of applications across different fields. As an example, in this context, there have been studies that employ CG simulations to assist in the design and development of display devices. Kiuchi and Koizumi conducted a simulation to reproduce mid-air image displays, evaluating the display's viewing angle and luminance attenuation rate [KK21]. Likewise, Matsubara et al. introduced a simulation for light field displays, successfully replicating the same visual experience as a real light field display [MAEG15]. Similar to these display devices, the grass pixel treated in this study require time for development and experiment, which involves the mapping of the color scale to the grass length. This study reproduces the grass pixel using CG simulations to assist in these efforts.

3. Grass display design and reproducing real environment

The purpose of this study is to simulate the color scale mapping by reproducing the grass pixel that composes the grass display in accurate color in the CG space. For reference and comparison experimentation of the grass pixel in the CG space, the grass pixel is created in the real space with reference to the paper by Tanaka et al. [TKM*23]. This section describes the hardware configuration of the grass pixel and the procedure for calculating the grass color.

3.1. Structure of grass display and grass pixel

Figure 2-(a) shows a relationship between the grass display and the grass pixel. The grass display consists of multiple grass pixels. Each grass pixel is designed based on pin display technology. The pin is moved up and down by the motor connected to the lead screw using the coupling. Artificial green grass is planted on top of the pin, and the grass pixel changes the green grass length as the pin is moved. Artificial yellow grass with slits for the green grass to pass through is fixed to the grass pixel, and the pin is moved, causing the green grass to change its length between the slits in the yellow grass.

Figure 2-(b) shows the principle of color recognition by the grass pixel. When observing the grass pixel, a user sees the color of the green and yellow grass as reflected light from the surrounding environment. At this time, the user observing the grass pixel from a sufficient distance away has difficulty distinguishing between green and yellow grass because the grass pixel is small. In this case, the user perceives them as a single average color that is additive mixed by spatial color mixing. In addition, as the green grass length changes, the ratio of the green grass in the area observed by the user changes. Thus, as shown in Figure 2-(b), the perceived color of the grass pixel changes depending on the green grass length.

3.2. Shape of the grass pixel

Figure 2-(c-1) shows the size and shape of the grass pixel designed and implemented in this study as the reference. A single blade of the green grass in the real space has a generally flat shape, and a single blade of the yellow grass is composed of an oval shape. The yellow grass is implemented by a three-dimensional (3D) printer and consists of a foundation and a yellow grass part. The foundation part is $33.5 \times 33.5 \times 15.0$ [mm] in size and has three slits 5.70 [mm] wide, and the yellow grass part extends from the top surface of the foundation part at a grass length of 10.0 [mm]. The green grass extends from the top of a 3D-printed pin part. The 3D-printed pin part is $24.0 \times 24.0 \times 65.0$ [mm] in size, with a length of 50 [mm]. An aluminum frame $110 \times 110 \times 300$ [mm] in size is implemented as a framework. As shown in Figure 2-(c-2), the green grass length is 0.00 [mm] at the base of the yellow grass. The green grass length changes from this point to a maximum of 15.00 [mm].

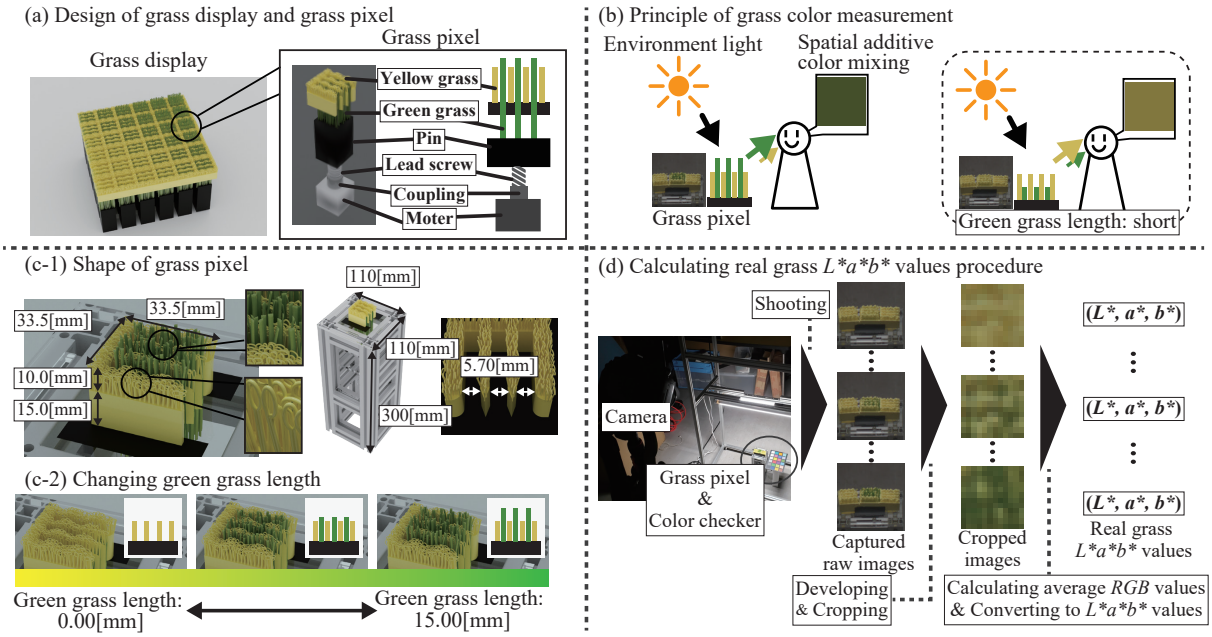

Figure 2: *Overview of the grass display and the grass pixel. (a) An image of the grass display and the grass pixel. (b) Principle of color recognition by grass pixel. On the left side, the green grass is longer and the user perceives green; on the right side, the green grass is shorter and the user perceives yellow. (c-1) Overall shape and size of the grass pixel. (c-2) The appearance of the grass pixel when the grass length of the artificial green grass is changed. (d) Procedure of shooting to calculate the real grass $L^*a^*b^*$ values.*

3.3. Grass color measurement of grass pixel

The procedure of measuring the grass color of the grass pixel is illustrated in Figure 2-(d). First, in preparation for photographing, the grass pixel is set up and a color checker is placed next to it. A camera position is fixed at the viewpoint desired for observing the grass pixel. For setting the camera's exposure, a gray card with 18% reflectance is captured from the camera position before shooting the grass pixel and the color checker. The camera's exposure settings are determined so that the light intensity of the captured gray card is in the middle of the luminance distribution. Next, the green grass length in the grass pixel is varied from 0.00 [mm] at regular intervals, and the grass pixel is shot in a raw image from the camera position and developed for each grass length. In development, the ACEScg color space [ACE21] with a wider color gamut is used instead of the standard RGB color space. Also, to reduce the effects of light changes during shooting that occur in real environments, color correction of the developed image is performed using the color checker based on 0.00 [mm] of the green grass length. The captured images of the grass pixel are cropped to the central region, and the average RGB values of the cropped area are subsequently calculated based on spatial color mixing. Finally, the obtained average RGB values are converted to values in CIE 1976 $L^*a^*b^*$ color space (L^*:luminance, a^*:redness, b^*:yellowness). In this study, $L^*a^*b^*$ values obtained from the grass pixel are defined as grass $L^*a^*b^*$ values, and the grass $L^*a^*b^*$ values in real space are defined as real grass $L^*a^*b^*$ values. The reason for using the $L^*a^*b^*$ color space is that the $L^*a^*b^*$ color space is more suitable for human color vision than the RGB color space, and quantitative comparisons can be made using the color difference formula CIEDE2000 ΔE^*_{00} [LCR01].

The following flow is used to convert from ACEScg color space to $L^*a^*b^*$ color space. First, the average RGB values in the ACEScg color space are transformed to XYZ values in CIE 1931 XYZ color space using the matrix in Eq. (1). Next, the white point in the ACEScg color space is approximated as a CIE daylight 6000K light source, and the white point is transformed to a CIE illuminant D_{50} light source. The white point transformation is obtained using the Bradford chromatic adaptation transform [Lam85]. The transformation formula is Eq. (2). Finally, the XYZ values in the XYZ color space are converted to the $L^*a^*b^*$ values in CIE 1976 $L^*a^*b^*$ color space.

$$\begin{bmatrix} X \\ Y \\ Z \end{bmatrix} = \begin{pmatrix} 0.662454 & 0.134004 & 0.156188 \\ 0.272229 & 0.674082 & 0.053690 \\ -0.00557465 & 0.00406073 & 1.01034 \end{pmatrix} \begin{bmatrix} R \\ G \\ B \end{bmatrix} \quad (1)$$

$$\begin{bmatrix} X' \\ Y' \\ Z' \end{bmatrix} = \begin{pmatrix} 1.03417 & 0.0168115 & -0.0374782 \\ 0.0216255 & 0.992232 & -0.0127228 \\ -0.00693874 & 0.0113271 & 0.813008 \end{pmatrix} \begin{bmatrix} X \\ Y \\ Z \end{bmatrix} \quad (2)$$

4. Method

This section first describes the method for constructing CG models of the grass pixel described in Section 3 and ambient light in the real space. Next, we explain the procedure for the grass $L^*a^*b^*$ values in the CG space via color correction. In this study, the grass $L^*a^*b^*$ values in the CG space are defined as CG grass $L^*a^*b^*$ values. The goal of reproducing the grass pixel and ambient light in the real space is to reduce the color difference between the CG grass $L^*a^*b^*$ values and the real grass $L^*a^*b^*$ values as shown in Figure 3. To achieve this goal, finally, we describe the method for calibrating material parameters of the color of the green and yellow grass in the CG space to correct the CG grass $L^*a^*b^*$ values.

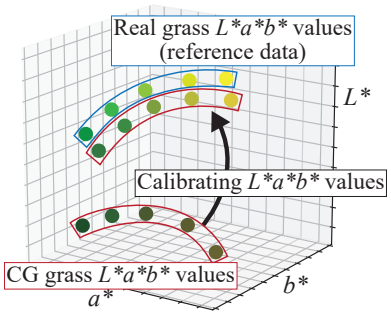

Figure 3: *Schematic diagram of the method. The CG grass $L^*a^*b^*$ values (red box) are corrected to the real grass $L^*a^*b^*$ values (blue box) by adjusting the color of the grass in the CG space.*

4.1. Setting CG models

As shown in Figure 4, a light source, a grass pixel CG model, a color checker CG model, and a virtual camera are placed in the CG space. For the grass pixel CG model, the yellow grass, the green grass, and an aluminum frame unit are implemented as CG models based on the geometry shown in Subsection 3.2. For the green grass, physical simulation is applied, varying from 0.00 [mm] to 15.00 [mm] as in the real space. The yellow and green grass are set as sub-surface scattering materials because they are translucent and non-metallic. For the color checker CG model, a texture is developed by referring to a datasheet of color checker $L^*a^*b^*$ values used in the real space. This texture is applied to a fully diffuse reflective flat object to implement the color checker CG model.

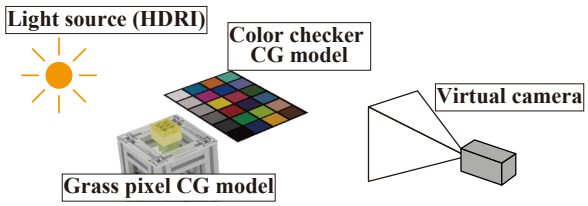

Figure 4: *Objects to be set in the CG space. Light source corresponding to real space ambient light, grass pixel and color checker CG models, and virtual camera are placed in the CG space.*

For the light source in the CG space, an omnidirectional High Dynamic Range image (HDRI) is used to set the environment light. Since HDRI has a wide dynamic range, it can retain information about light in the real space without missing general information, thus reproducing the effects of real space ambient light more accurately [RHD*10]. In the HDRI acquisition, an omnidirectional camera is installed at the same location where the grass pixel is installed in the real space, and raw images to merge omnidirectional HDRI are taken. The virtual camera in the CG space is set to the color space during the rendering process. In this study, the ACEScg color space is adopted as the color space for rendering output and the working color space. Finally, the above elements are placed in the CG space. A color checker CG model is placed at the same height as the top of the grass pixel CG model, and HDRI environment light is placed. Finally, a virtual camera that renders is placed in the same camera position from which the grass pixel is shot in the real space.

4.2. From rendering to CG grass $L^*a^*b^*$ values calculation

Figure 5-(a) shows an overview of the flow from a render process to calculating the CG grass $L^*a^*b^*$ values. First, the render process is performed in the ACEScg color space from the virtual camera changing the green grass length. Next, the rendered image is applied a color correction based on the color checker. The purpose of this color correction is to modify for color difference between the CG grass $L^*a^*b^*$ values and the real grass $L^*a^*b^*$ values caused by white balance and exposure settings. The color checker used as a reference is a color checker that is placed next to the grass pixel during the capture of the grass pixel in the real space. The rendered images are applied color correction using 24 patches of the reference color checker and the color checker included in the rendered images. Then, the color-corrected image is cropped in a square region about the center of the grass pixel. In addition, the average RGB values are calculated based on the principle of spatial additive color mixing for the cropped area. Finally, the CG grass $L^*a^*b^*$ values are calculated from the obtained RGB values using the procedure explained in Subsection 3.3.

4.3. Estimating material parameters using optimization

Since the purpose of this method is to reduce the difference between the real grass $L^*a^*b^*$ values and the CG grass $L^*a^*b^*$ values, which are the average color of the cropped area, the scattering color of the green and yellow grass that more affect the CG grass $L^*a^*b^*$ values than other material parameters is estimated using an optimization algorithm. In this study, the used grass lengths are limited to the minimum (green grass length: 0.0 [mm]), where the influence of yellow grass is large, and the maximum (green grass length: 15.0 [mm]), where the influence of green grass is large. Figure 5-(b) shows a summary of this calibration.

We use a genetic algorithm (GA) as an optimization algorithm. GA is used because it avoids the possibility of falling into local solutions more than the general gradient method. A flow chart of the algorithm is shown in Figure 5-(c), and Table 1 shows variables used in this optimization. The correct value is the real grass $L^*a^*b^*$ values Lab_L obtained from the grass pixel of green grass length L shot in the real space, and the input value is the CG grass $L^*a^*b^*$ values $\hat{Lab}_L(M_Y, M_G)$ obtained by rendering the grass pixel of the green grass length L, the scattering color M_G for the green grass, and the scattering color M_Y for the yellow grass. Next, the color difference ΔE^*_{00} between the correct value Lab_L and the input value $\hat{Lab}_L(M_Y, M_G)$, is calculated for each green grass length D. However, as explained above, the green grass length used in the calculations is limited to $D \in \{0.00, 15.00[\text{mm}]\}$. The inverse of these sums of squares is used as the objective function in Eq. (3), where ϵ is a tiny constant value. This optimization is implemented as a maximization problem.

$$G(M_Y, M_G) = \frac{1}{\sum_{l \in D}(\Delta E^*_{00}(Lab_l, \hat{Lab}_l(M_Y, M_G)))^2 + \epsilon} \tag{3}$$

The termination condition is set when the color difference is below the ΔE^*_{00} value $\epsilon_{\Delta E}$ in all grass length or when the maximum number of generations is completed. From the viewpoint of computational complexity, the crop process is implemented by limiting the rendering area.

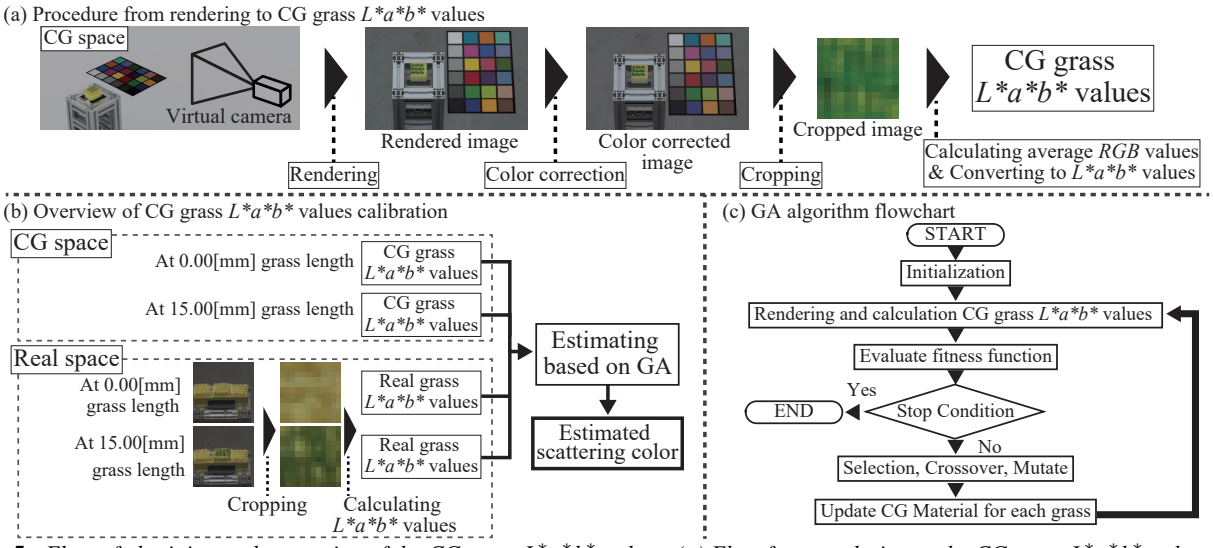

Figure 5: *Flow of obtaining and correcting of the CG grass $L^*a^*b^*$ values. (a) Flow from rendering to the CG grass $L^*a^*b^*$ values. Color correction is performed on the rendered image, and then the CG grass $L^*a^*b^*$ values are acquired in the same way as in the real space. (b) Overall image of the correction of the CG grass $L^*a^*b^*$ values. (c) Flowchart of GA algorithm.*

Table 1: *GA algorithm variables*

variables	describes
M_Y	yellow grass scattering color (r, g, b)
M_G	green grass scattering color (r, g, b)
D	the set of the green grass length
Lab_l	the real grass $L^*a^*b^*$ values at green grass length l
$\hat{Lab}_l(M_Y, M_G)$	the CG grass $L^*a^*b^*$ values with scatter color M_Y, M_G at green grass length l
ϵ	constant value

5. Experiment

The objectives of this experiment are twofold.

1. To confirm the color difference of the color of the grass pixel at each grass length between the real and CG space.
2. To confirm the effectiveness of the results of the color scale mapping for the grass pixel in the CG space.

5.1. Experimental condition

This experiment was conducted in an International Organization for Standardization (ISO) 3664:2009 environment [ISO09]. This environment was chosen because it was suitable for the color evaluation conditions [SS97] used in another experiment by Tanaka et al. [TKM*23]. The experiment was conducted in a room with no external light coming in that met the ISO color evaluation requirements, and two LEDs for color evaluation (ECL-LD2EGN-L3A, 5000K, Ra>95) were installed at a height of 0.50 [m] to keep the illuminance on the top surface of the grass pixel at 2000±250 [lux]. In addition, a classroom was prepared as another lighting environment to confirm the difference in results depending on the environment. Figure 6 shows the experiment setup in both environments.

5.1.1. Grass color measurement in the real space

The hardware configuration of the grass pixel was a stepper motor (SM-42BYG011-25, 200 [steps/rotation]), a microcontroller (Teensy 4.2) for motor control, and a stepper motor driver (DRV8825). A lead screw with coupling (length: 100.0 [mm], pitch: 6.0 [mm], lead: 6.0) was used, and pin and yellow grass were 3D printed (Creality Ender-3 Pro) using black and yellow filament (ANYCUBIC Filament, material: polylactic acid (PLA), diameter: 1.75±0.02 [mm]). The overall shape was described in Subsection 3.2.

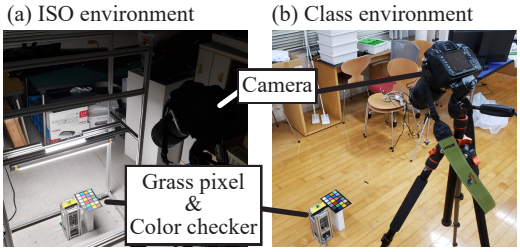

Figure 6: *The experimental setup in (a) ISO environment, and (b) classroom environment.*

A Nikon D7000 digital camera and an AF Zoom-Nikkor 35-70mm F2.8S lens were used to capture raw images of the grass pixel. Using an 18% gray card (GIN-ICHI, SILK GRAY CARD ver.2), the camera settings were fixed at the camera's aperture of f/5.6, shutter speed of 1/25, ISO 100, and focal length of 35 mm for the ISO environment and the camera's aperture of f/5.6, shutter speed of 1/6, ISO 100, and focal length of 35 mm for the classroom environment. During the shooting, a DataColor SpyderCheckr 24 color checker was set up near the grass pixel. The raw images were developed as 16-bit TIFF images in ACEScg color space with a resolution of 2470×1636 [px] using Another Raw Therapee. The color temperature and tint of the ISO environment were 4611 and 0.907, and the color temperature and tint of the classroom environment were 3503 and 0.755. The camera position in shooting was determined as shown in Figure 7-(a), with distance $d = (1.0, 2.0, 3.0[\mathrm{m}])$, and angle $\theta = (0, 30, 60, 90[\mathrm{deg}])$. Since the results of other studies [TKM*23] showed that the effect of camera

height was smaller than that of θ and d, the height of the camera was fixed at 1.7 [m]. Figure 7-(b) shows the actual images with d = 1.0 and θ varied to $(0, 30, 60, 90[\text{deg}])$. The green grass length in the grass pixel varied from 0.0 [mm] to 15.0 [mm] in steps of 0.75 [mm], and the real grass $L^*a^*b^*$ values were obtained using the procedure in Subsection 3.3. A Ricoh Theta Z1 was used as the omnidirectional camera to capture omnidirectional raw images. The omnidirectional raw images had a resolution of 7296×3648 [px] and were merged with Photoshop to create HDRI.

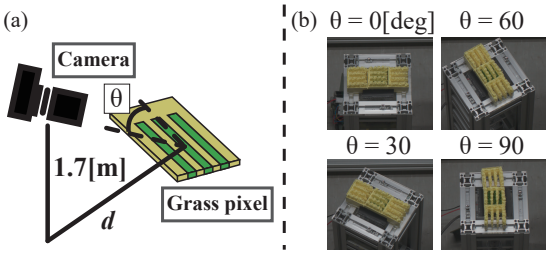

Figure 7: *Camera and the grass pixel positioning. (a) Imaged figure. (b) Photographs at* $\theta = (0, 30, 60, 90[deg])$ *with* $d = 1.0[m]$.

5.1.2. Grass color measurement in the CG space

Houdini version 19.0.561 by SideFX, Inc. was used as the 3DCG software, and Redshift version 3.5.4 by Maxon Computer GmbH, Inc. served as the renderer. The rendered image had a resolution of 2470×1636 [px], and its file format was a 16-bit TIFF. The sample count of rays per pixel was set to 1024. Regarding the execution environment, we utilized both an Intel Core i7-11700 and NVIDIA Geforce RTX 4070 machine and an Intel Core i7-7700K and NVIDIA Geforce RTX 3090 Ti machine. In the grass pixel CG model, the green grass length was varied from 0.0 [mm] to 15.00 [mm] at 0.75 [mm] intervals. The height of the virtual camera was fixed at 1.7 [m], d was set at $(1.0, 2.0, 3.0[\text{m}])$, and θ was set at $(0, 30, 60, 90[\text{deg}])$. The material parameters of the green and yellow grass in the CG space were defined using Redshift's material shader. Since the green grass was made of polypropylene, studies estimating the specular reflection parameters of polypropylene were used as a reference for an index of refraction (IOR) and reflection roughness [NDM05]. The yellow grass was made of polylactide, and the IOR and reflective roughness values of the yellow grass were determined using the plastic preset in Redshift's material shader. Table 2 details the specific material parameters. Additionally, the texture for the color checker was created in Photoshop with the SpyderCheckr 24 datasheet as a reference.

The programs of rendering, calculating the CG grass $L^*a^*b^*$ values, and estimating material parameters were developed in Python 3.7. PlantCV 3.14.3 was employed to apply the color correction using the color checker, and PyGAD 2.18.1 facilitated the implementation of the GA. When setting up the parameters of the GA, the maximum number of generations in the search was capped at 100, the number of individuals was set at 50, and constant value ϵ was set at $1.0 \times e^{-7}$. The color difference of the termination condition $\epsilon_{\Delta E}$ was set at 1.0. The search range for solutions was defined around a specific range, namely ±0.5 based on yellow (1.0, 1.0, 0.0) for the yellow grass and bright green (0.5, 1.0, 0.5) for the green one. However, the search range for scattering color was restricted not to exceed the [0.0, 2.0] interval. The CG grass $L^*a^*b^*$ values were obtained for each green grass length in the procedure of Subsection 4.2, using the grass pixel model with the scattering colors estimated by the GA for each camera position. In this case, the average value of ΔE^*_{00} for 24 patches of the color checker between real space and CG space was less than 3.0 in all environments and camera positions.

Table 2: *Material parameters for the yellow and green grass*

	Green grass	Yellow grass
reflection model	Cook-Torrance	
reflection roughness	0.0429	0
index of refraction	1.518	1.49
sub-surface scattering radius	0.1	0.1

5.2. Results of color difference between the real and CG space

The color difference between the grass pixel in the real and CG space was calculated in this experiment to evaluate the reproducibility of the color of the grass pixel in the CG space. The real grass $L^*a^*b^*$ values and the CG grass $L^*a^*b^*$ values were measured at each grass length for each environment, and each camera position. Then, the color difference ΔE^*_{00} between the real grass $L^*a^*b^*$ values and the CG grass $L^*a^*b^*$ values at each grass length was calculated for each environment, and each camera position.

For the real grass $L^*a^*b^*$ values and the CG grass $L^*a^*b^*$ values measured at each grass length, a 3D plot of the results at each camera position in the ISO environment is shown in Figure 8. In Figure 8, the CG grass $L^*a^*b^*$ values are plotted in red and the real grass $L^*a^*b^*$ values are plotted in blue. The results show that the shape of the graph of the CG grass $L^*a^*b^*$ values were close to the real grass $L^*a^*b^*$ value at all camera positions (d, θ). Thus, the grass pixel in the CG space reproduced the same transition of the $L^*a^*b^*$ values as the grass pixel in the real space.

The color difference between the real grass $L^*a^*b^*$ values and the CG grass $L^*a^*b^*$ values was evaluated. Table 3 shows the mean and maximum color difference between the real grass $L^*a^*b^*$ values and the CG grass $L^*a^*b^*$ values per green grass length at each camera position in the ISO and classroom environments. In this experiment, the maximum value of ΔE^*_{00} for each grass length was below 3.0 for all camera positions in both environments. A color difference ΔE^*_{00} of 3.0 is the color tolerance for commercial printed materials in the ANSI and Committee for Graphic Arts Technologies Standards (CGATS) [Com14]. Therefore, this result means that the grass pixel reproduced in the CG space were close sufficient in color to the grass pixel in the real space.

Table 3: *Average and maximum values of color difference at each camera position and at each grass length of the green grass.*

		The ISO environment			The classroom environment		
		1.0[m]	2.0	3.0	1.0[m]	2.0	3.0
0[deg]	ave.	0.93	1.33	1.07	1.22	1.44	1.34
	max.	1.26	2.01	1.67	1.57	2.88	2.22
30	ave.	0.74	0.96	1.39	1.28	0.97	1.75
	max.	1.23	1.40	1.94	2.03	1.81	2.66
60	ave.	1.40	1.18	1.26	1.32	1.17	1.24
	max.	1.73	1.95	2.11	1.93	2.42	2.68
90	ave.	2.06	1.95	1.59	2.11	1.07	1.11
	max.	2.46	2.41	2.26	2.35	1.59	1.57

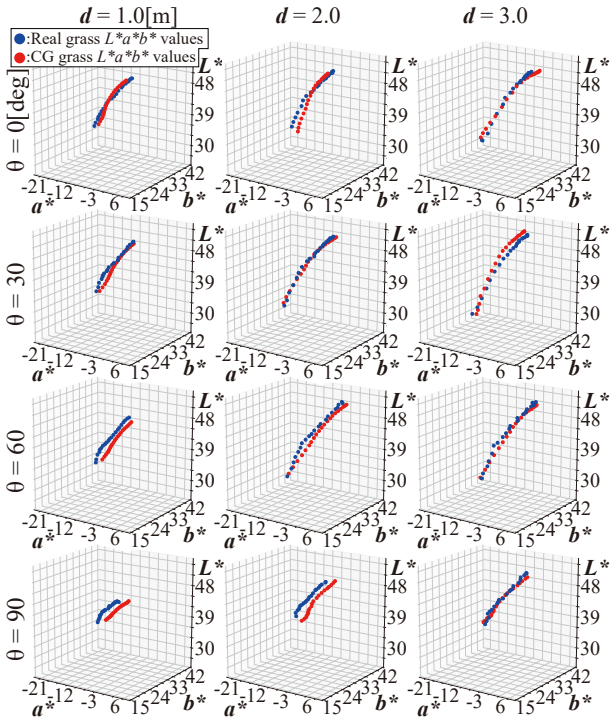

Figure 8: *Graph of the real grass $L^*a^*b^*$ values and the CG grass $L^*a^*b^*$ values.*

From the above results, the CG simulation of the grass pixel proposed in this study generally reproduces the color of the grass pixel in the real space.

5.3. Results of color scale mapping

5.3.1. Color scale mapping method overview

Here, we obtain the grass length corresponding to each level using the color scale mapping for the grass pixel in the CG space. Then, we reveal whether the resulting grass lengths of the CG space are valid for controlling the color scale of the grass pixel in the real space. In this paper, we focus on a five-level color scale mapping method based on another experiment by Tanaka et al. [TKM*23].

We explain the overview of the color scale mapping method of the grass pixel as shown in Figure 9. This method requires grass $L^*a^*b^*$ values at regular intervals of the grass length from minimum to maximum. These grass $L^*a^*b^*$ values are measured from a certain perspective such as those obtained in Subsection 5.2. Using these measured grass $L^*a^*b^*$ values, a reference $L^*a^*b^*$ value for each level G_n is calculated $(n = 0,1,2,3,4)$. G_0 and G_4 are defined as grass $L^*a^*b^*$ values when the grass lengths are minimum and maximum, respectively. G_1, G_2 and G_3 are $L^*a^*b^*$ values on the G_0 and G_4 line segment in the $L^*a^*b^*$ color space and satisfy the following equation 4. Thus, the reference grass $L^*a^*b^*$ value G_k is obtained.

$$\Delta E^*_{00}(G_0, G_n) = \frac{n}{4}\Delta E^*_{00}(G_0, G_4) \quad (n = 1,2,3) \tag{4}$$

Next, the color scale mapping method finds the grass $L^*a^*b^*$ value corresponding to G_n. A color tolerance is set for each G_n $(n = 1,2,3)$ as a blue ellipse in Figure 9. In the color scale mapping method, the color tolerance is defined as 3.0 based on the CGATS category of the color tolerance [Com14]. When a measured grass $L^*a^*b^*$ value is within the color tolerance of G_n, the perceived color of the measured grass $L^*a^*b^*$ value is considered the same as the perceived color of G_n. Finally, when G_1, G_2, and G_3 correspond to the measured grass $L^*a^*b^*$ values, the color scale of the grass pixel can be set.

Finally, the color scale mapping method generates a list of grass lengths corresponding to the real grass $L^*a^*b^*$ values included in the color tolerance for each Gn. In addition, levels 0 and 4 are assigned to the minimum and maximum grass length, respectively. However, when a color tolerance of G_n includes another reference $L^*a^*b^*$ value $G_i (i \neq n)$, the perceived color of G_n and G_i is the same, so the color scale mapping is considered to be impossible. Since the color tolerance is set to 3, the color scale mapping method cannot provide the grass lengths based on the color scale when the color difference between G_0 and G_4 is less than 12.

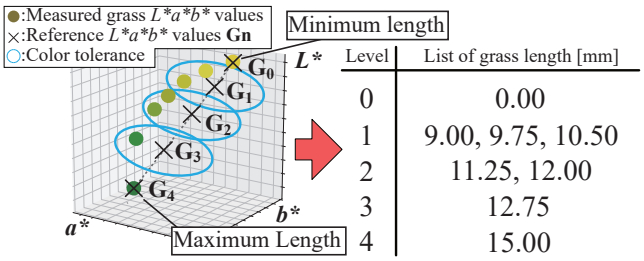

Figure 9: *Example of color scale mapping method*

5.3.2. Evaluation results of color scale mapping

We reveal whether the results of the color scale mapping in the CG space are effective in controlling the color scale of the grass pixel in the real space.

First, based on each camera position, the color scale mapping is performed on the real and CG grass $L^*a^*b^*$ values from the minimum to maximum grass length, respectively. In the experiments, we use the real and CG grass $L^*a^*b^*$ values obtained in Subsection 5.2. Then, the color scale mapping method provides a list of grass lengths corresponding to the five-level color scale based on the real and CG space, respectively.

As a specific example of the list of the grass lengths, Table 4 shows the results of the color scale mapping at $(d, \theta) = (3.0, 0)$ in the classroom environment based on the real and CG space, respectively. In the experiments, we use the grass length corresponding to the CG grass $L^*a^*b^*$ values with the smallest ΔE^*_{00} from each reference $L^*a^*b^*$ values G_n. This grass length for each G_n is defined as $L_{cg\_n} (n = 0,1,2,3,4)$. As shown in Table 4, L_{cg_n} is indicated by a red color for each level. In this case, L_{cg_n} is also included in the list of the grass lengths in the real space at each level as indicated by the underlines in Table 4. In other words, the relationship between the levels of the color scale and the grass length obtained by the color scale mapping in the CG space can be used in the real-space grass pixel.

In these experiments, to simplify the experimental conditions, we evaluate the effectiveness of the color scale mapping in the CG space at $(d, \theta) = (1.0, 0), (2.0, 0), (3.0, 0)$ based on the ISO and classroom environments.

Table 4: *Example of color scale mapping result*

Level n	list of grass lengths in CG space [mm]	list of grass lengths in real space [mm]
0	0.00	0.00
1	9.00, 9.75, 10.50	7.50, 8.25, 9.00, 9.75, 10.50
2	11.25	11.25, 12.00
3	12.00, 12.75, 13.50	12.75, 13.50
4	15.00	15.00

As a result, we revealed that the grass pixel in the real space could be color-scale controlled by using the grass lengths L_{cb_n} obtained by the color scale mapping in the CG space. Specifically, for five of the six experimental conditions, all levels of L_{cg_n} were included in the list of the grass lengths in the real space.

For example, here is the successful result at $(d,\theta) = (2.0,0)$ in the ISO environment through Figure 10-(a). Dots represent the real grass $L^*a^*b^*$ values. In addition, cross marks represent the reference $L^*a^*b^*$ values G_n calculated based on these real grass $L^*a^*b^*$ values, and blue ellipse represents the color tolerance of each G_n. In this experimental condition, L_{cg_n} was 0.00, 6.75, 10.50, 12.75, and 15.00 [mm] in order of color scale level. In this case, the dots of the real grass $L^*a^*b^*$ values corresponding to the grass lengths $L_{cg\_n}(n = 1,2,3)$ are shown in red in Figure 10-(a). This figure shows the red dots are included in the color tolerance of each G_n. Therefore, the color scale mapping results of the CG space are useful to the grass pixel in the real space. Moreover, as shown in Figure 10-(b), the colors of the real-space grass pixel corresponding to L_{cg_n} represent five levels of the color scale visually.

However, when (d,θ) was $(2.0,0)$ in the classroom environment, all L_{cg_n} could not be included in the real-space list of the grass lengths. L_{cg_n} was 0.00, 9.00, 11.25, 12.75, and 15.00 [mm] in order of color scale level, and 12.75 [mm] of L_{cg_3} was not included in the real-space list of the grass lengths. However, the color difference between the reference $L^*a^*b^*$ values G_3 and the real grass $L^*a^*b^*$ values corresponding to L_{cg_3} was 3.45. In other words, the real grass $L^*a^*b^*$ values of L_{cg_3} were located almost at the boundary of the G_3 color tolerance. Moreover, as shown in Figure 10-(c), the real-world grass pixel with the grass length L_{cg_n} could display the color based on the color scale visually. Therefore, we revealed that the color scale mapping system results of the CG space could be effective for the color-scale control of the real-space grass pixel in our experimental conditions.

6. Limitation

The system proposed in this study requires an image of a grass pixel taken in the real space for each camera position in order to estimate the color of the grass. This is a major problem for future applications that require real-space images of grass pixel for evaluation in the CG space. To solve this problem, for example, material-specific bidirectional scattering surface reflectance distribution function could be measured and applied to the grass pixel CG model [JMLH01].

7. Conclusion

This paper proposed a simulation system using CG techniques for the grass pixel. By recreating the ambient light and the grass pixel in the real space into the CG space, there is potential to reduce the experimental workload required for the color scale mapping of the

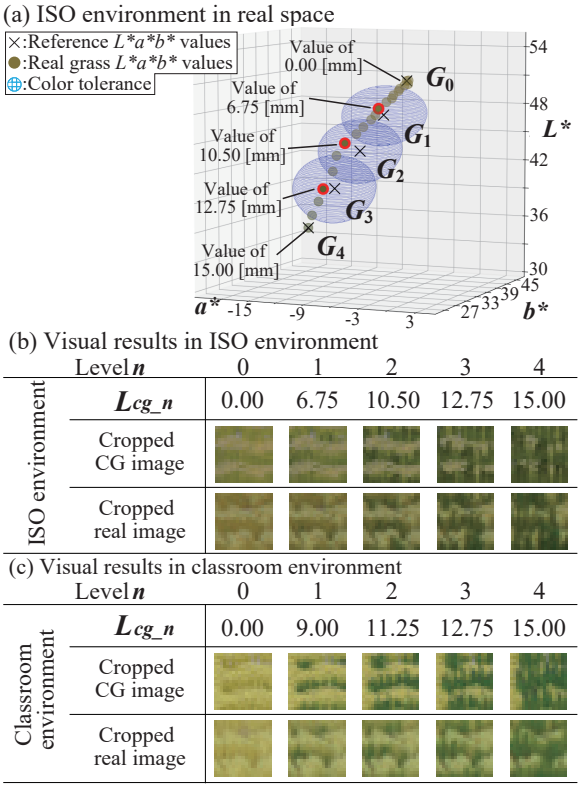

Figure 10: *Result of color scale mapping experiments. (a) Real grass $L^*a^*b^*$ values and Reference $L^*a^*b^*$ values at $(d,\theta) = (2.0,0)$ in the ISO environment. (b)(c) Images of the grass pixel in the both real and CG space according to L_{cg_n} in the ISO and classroom environment, respectively.*

grass pixel. This system can also be applied to reflective devices using the principle of spatial additive color mixing and to the reproduction of color mixing using other colors.

In our study, we prepared an omnidirectional HDRI of ambient light in real space, images of a color checker and a grass pixel taken at the observation position in real space as digital data for calibrating CG space. By using these data, the grass pixel CG model and the light source were set in the CG space, and the CG model of the grass pixel could be calibrated based on the GA algorithm. We confirmed that the grass pixel in the CG space reproduced the color of the grass pixel in the real space. We also revealed that the results of the color scale mapping system derived from the CG simulation could be applied to the color scale control of the grass pixel in the real space.

As future work, we are going to work on data reduction needed to calibrate the color of the grass material and conduct experiments in more environments. In particular, experiments on varying the vertical angle at which a camera observes the grass pixel are important. The slits in the grass pixel possibly affect the measured color by observing from the top. This potential effect on color measurement requires verification of color reproducibility using CG simulation.

8. Acknowledgements

This work was supported by JST SPRING, Grant Number JPMJSP2124.

References

[ACE21] St 2065-1:2021 - smpte standard - academy color encoding specification (aces). *ST 2065-1:2021* (2021), 1–20. doi:10.5594/SMPTE.ST2065-1.2021. 3

[Com14] Committee for Graphic Arts Technologies Standards (CGATS): *Graphic Technology-Printing Tolerance and Conformity Assessment*. Tech. rep., CGATS TR 016-2014, 2014. 6, 7

[Dis15] Disney Research and a student team at ETH Zürich: Beachbot. http://www.beachbot.ch/, 2015. Accessed: (Aug-2023). 1, 2

[DWPF15] Du R., Wills K. R., Potasznik M., Froehlich J. E.: Atmosphere: Representing space and movement using sand traces in an interactive zen garden. In *Proceedings of the 33rd Annual ACM Conference Extended Abstracts on Human Factors in Computing Systems* (New York, NY, USA, 2015), CHI EA '15, Association for Computing Machinery, pp. 1627–1632. doi:10.1145/2702613.2732771. 2

[Ecl14] Eclipse Digital Media: Knowsle safari. https://www.eclipsedigitalmedia.co.uk/project/knowsley-safari/, 2014. Accessed: (Aug-2023). 1

[GL21] Guida M., Leoncini P.: Regional aircraft interiors evaluation in a real time ray-traced immersive virtual environment. In *Augmented Reality, Virtual Reality, and Computer Graphics: 8th International Conference, AVR 2021, Virtual Event, September 7–10, 2021, Proceedings 8* (2021), Springer International Publishing, pp. 483–498. doi:https://doi.org/10.1007/978-3-030-87595-4_35. 2

[Gov20] Government of Japan: Rice paddy art. https://www.gov-online.go.jp/eng/publicity/book/hlj/html/202011/202011_05_en.html, 2020. Accessed: (Aug 2023). 1

[GSEM18] Gentile V., Sorce S., Elhart I., Milazzo F.: Plantxel: Towards a plant-based controllable display. In *Proceedings of the 7th ACM International Symposium on Pervasive Displays* (New York, NY, USA, 2018), PerDis '18, Association for Computing Machinery. doi:10.1145/3205873.3205888. 2

[HPC*] Heydarian A., Pantazis E., Carneiro J. P., Gerber D., Becerik-Gerber B.: *Towards Understanding End-User Lighting Preferences in Office Spaces by Using Immersive Virtual Environments*. pp. 475–482. doi:10.1061/9780784479247.059. 2

[ISO09] ISO 3664:2009: Viewing conditions – Graphic technology and photography. https://www.iso.org/standard/43234.html, 2009. Accessed: (Aug 2023). 5

[JMLH01] Jensen H. W., Marschner S. R., Levoy M., Hanrahan P.: A practical model for subsurface light transport. In *Proceedings of the 28th Annual Conference on Computer Graphics and Interactive Techniques* (New York, NY, USA, 2001), SIGGRAPH '01, Association for Computing Machinery, pp. 511–518. doi:10.1145/383259.383319. 8

[KK21] Kiuchi S., Koizumi N.: Simulating the appearance of mid-air imaging with micro-mirror array plates. *Computers & Graphics 96* (2021), 14–23. doi:https://doi.org/10.1016/j.cag.2021.02.007. 2

[Lam85] Lam K. M.: Metamerism and color constancy. *Ph. D. Thesis, University of Bradford* (1985). 3

[LCR01] Luo M. R., Cui G., Rigg B.: The development of the cie 2000 colour-difference formula: Ciede2000. *Color Research & Application 26*, 5 (2001), 340–350. doi:https://doi.org/10.1002/col.1049. 3

[MAEG15] Matsubara R., Alpaslan Z. Y., El-Ghoroury H. S.: Light field display simulation for light field quality assessment. In *Stereoscopic Displays and Applications XXVI* (2015), Holliman N. S., Woods A. J., Favalora G. E., Kawai T., (Eds.), vol. 9391, International Society for Optics and Photonics, SPIE, p. 93910G. doi:10.1117/12.2083438. 2

[MN12] Minuto A., Nijholt A.: Growing grass: A smart material interactive display, design and construction history. In *Proceedings of the 1st Workshop on Smart Material Interfaces: A Material Step to the Future* (New York, NY, USA, 2012), SMI '12, Association for Computing Machinery. doi:10.1145/2459056.2459063. 2

[MZS*19] Min X., Zhang W., Sun S., Zhao N., Tang S., Zhuang Y.: Vpmodel: High-fidelity product simulation in a virtual-physical environment. *IEEE Transactions on Visualization and Computer Graphics 25*, 11 (2019), 3083–3093. doi:10.1109/TVCG.2019.2932276. 2

[NDM05] Ngan A., Durand F., Matusik W.: Experimental Analysis of BRDF Models. In *Eurographics Symposium on Rendering (2005)* (2005), Bala K., Dutre P., (Eds.), The Eurographics Association. doi:10.2312/EGWR/EGSR05/117-126. 6

[NMI*20] Nagafuchi R., Matoba Y., Ikematsu K., Ishii A., Kawahara Y., Siio I.: Polka: A water-jet printer for painting on the grounds. In *Proceedings of the International Conference on Advanced Visual Interfaces* (New York, NY, USA, 2020), AVI '20, Association for Computing Machinery. doi:10.1145/3399715.3399817. 1, 2

[RHD*10] Reinhard E., Heidrich W., Debevec P., Pattanaik S., Ward G., Myszkowski K.: *High dynamic range imaging: acquisition, display, and image-based lighting*. Morgan Kaufmann, 2010. 4

[RPH*19] Robinson S., Pearson J., Holton M. D., Ahire S., Jones M.: Sustainabot - exploring the use of everyday foodstuffs as output and input for and with emergent users. In *Proceedings of the 2019 CHI Conference on Human Factors in Computing Systems* (New York, NY, USA, 2019), CHI '19, Association for Computing Machinery, pp. 1–12. doi:10.1145/3290605.3300456. 2

[Sad14] Sade G.: Aesthetics of urban media façades. In *Proceedings of the 2nd Media Architecture Biennale Conference: World Cities* (New York, NY, USA, 2014), MAB '14, Association for Computing Machinery, pp. 59–68. doi:10.1145/2682884.2682887. 1

[SS97] Sato T., Sato I.: Requirements governing light sources used for color evaluation. In *Proceedings of the 8th Congress of the International Colour Association* (1997), vol. 1, pp. 415–418. 5

[STH*14] Sugiura Y., Toda K., Hoshi T., Kamiyama Y., Igarashi T., Inami M.: Graffiti fur: Turning your carpet into a computer display. In *Proceedings of the 27th Annual ACM Symposium on User Interface Software and Technology* (New York, NY, USA, 2014), UIST '14, Association for Computing Machinery, pp. 149–156. doi:10.1145/2642918.2647370. 2

[STK*17] Sugiura Y., Toda K., Kikuchi T., Hoshi T., Kamiyama Y., Igarashi T., Inami M.: Grassffiti: Drawing method to produce large-scale pictures on conventional grass fields. In *Proceedings of the Eleventh International Conference on Tangible, Embedded, and Embodied Interaction* (New York, NY, USA, 2017), TEI '17, Association for Computing Machinery, pp. 413–417. doi:10.1145/3024969.3025067. 2

[TKM*23] Tanaka K., Kato Y., Mizuno A., Mikawa M., Fujisawa M.: Dynamic grass color scale display technique based on grass length for green landscape-friendly animation display. *Scientific Reports 13*, 1 (Jan 2023), 260. doi:10.1038/s41598-022-27183-x. 1, 2, 5, 7

[TMF21] Tanaka K., Mikawa M., Fujisawa M.: Natural landscape-friendly animation display technique using shape-changing artificial grass system. In *2021 IEEE International Conference on Systems, Man, and Cybernetics (SMC)* (2021), pp. 2549–2554. doi:10.1109/SMC52423.2021.9659032. 1, 2